A Thermo-Electrochemical Model of 18.5 V/50 Ah Battery Module for Railway Vehicles

Jihun Song[1†], Hyobin Lee[1†], Suhwan Kim[1], Dongyoon Kang[1], Seungwon Jung[1], Hongkyung Lee[1,2], Tae-Soon Kwon[3*] and Yong Min Lee[1,2*]

[1]Department of Energy Science and Engineering, Daegu Gyeongbuk Institute of Science and Technology (DGIST), Daegu, South Korea, [2]Energy Science and Engineering Research Center, Daegu Gyeongbuk Institute of Science and Technology (DGIST), Daegu, South Korea, [3]Railroad Safety Research Division, Korea Railroad Research Institute (KRRI), Uiwang, South Korea

We developed a thermo-electrochemical model of a 50 Ah pouch-type lithium-ion cell and utilized a cell model to build an 18.5 V/50 Ah module to analyze the thermal behavior under various operating conditions and design cooling systems for optimal operating temperature ranges. Specifically, the heat generated by electrochemical reactions was simulated through an electrochemical cell model, and then the calculated heat was coupled with a heat transfer model reflecting the actual 3D structure of the cell. By fitting two temperature-dependent parameters, i.e., the chemical diffusion coefficient and exchange current density, the model accurately estimated the electrochemical and thermal properties with errors less than 3%, even under wide temperature (25°C, 35°C, and 45°C) and C-rate (0.5, 1, 2, and 5C) conditions. Based on this reliable cell model, we built an 18.5 V/50 Ah module model with five cells in series to simulate both the amount of heat generated and the required heat sink. Finally, both the cell and module models were used to predict the electrochemical and thermal behaviors under actual wireless tram operations in Turkey. The model results were compared with experimental results to confirm their reliability.

Keywords: thermo-electrochemical model, battery module, exchange current density, diffusion coefficient, cooling system

INTRODUCTION

Various types of electric vehicles (xEVs), including hybrid electric vehicles (HEVs), plug-in hybrid electric vehicles, and battery electric vehicles (BEVs), have been developed owing to large-format, cost-effective, and high energy density lithium-ion batteries (LIBs). Furthermore, strict environmental policies in many countries have accelerated the growth of the global xEV market. Because of this soft landing of EVs, several attempts have been made to install LIBs in railway vehicles (Okui et al., 2010; Konishi and Tobita, 2012; Ciccarelli et al., 2014). However, the frequent incidents of accidental fires or explosions involving EVs on the road are major obstacles to the battery-based electrification of railway vehicles. Considering that there are more passengers on railway vehicles running in isolated spaces, such as tunnels or underground, ensuring the safety of LIBs should be the top priority for electric railway vehicles.

In this regard, it is essential to understand the reasons behind the accidental fire or explosion of EVs to develop practical solutions. Many researchers have attempted to determine the causes and mechanisms of thermal runaway (TR), a process that frequently occurs in LIBs. TR can be divided

into three stages (Feng et al., 2018). In the first stage, the voltage decreases slowly along with a slight increase in temperature, both of which go relatively undetected. However, when the voltage starts to decrease rapidly and the temperature rises significantly, the second stage begins. If the temperature reaches a critical point, such as the meltdown temperature of the separator, the LIB combusts or explodes. To avoid TR, it is necessary to control the temperature of the LIB so that TR does not progress beyond the first stage.

For this purpose, appropriate cooling systems should be installed for LIB modules and packs in various vehicles. However, with limited thermocouples on the surface of cells or parts, managing the overall thermal behavior of modules or packs is difficult. In particular, under harsh operating conditions such as a high cutoff voltage, C-rate, and environmental temperature, accurately predicting the heat generated by electrochemical reactions has become more challenging with limited measured temperature data. To deal with this issue, theoretical simulations have been reported by coupling thermal and electrochemical models of LIB systems (Chen and Evans, 1994; Pals and Newman, 1995; Verbrugge, 1995; Rao and Newman, 1997; Gu and Wang, 2000; Song and Evans, 2000; Srinivasan and Wang, 2003; Kumaresan et al., 2008; Guo et al., 2011). Many studies have applied these theories to actual batteries (Chen and Evans, 1993; Chen et al., 2005; Wu et al., 2012; Kim et al., 2014; Lai et al., 2015; Zhao et al., 2015; Basu et al., 2016; Bahiraei et al., 2017; Jeong et al., 2019; Liang et al., 2019; Liang et al., 2020; Wang et al., 2021).

Kim et al. developed a thermo-electrochemical model of a prismatic-type cell of 50 Ah and predicted the temperature. However, the main parameters, i.e., the diffusion coefficient and rate constant (exchange current density), were set as constant values despite their dependence on the temperature and state of lithiation (SOL). Their simulated electrochemical performance was not verified with experimental results. Moreover, their model was not extended to a module or pack scale, which is essential for practical applications (Kim et al., 2014). Bahiraei et al. and Liang et al. developed thermo-electrochemical models for modules with pouch-type 10 Ah LIB cells for HEV applications. However, it is difficult to apply these models to large-format and high energy density LIB modules for railway vehicles because their cell designs are totally different. (Bahiraei et al., 2017; Liang et al., 2020). Owing to the increased concerns over the safety of battery systems in railway vehicles, more realistic battery module models based on large-format and high energy density LIB cells should be developed and utilized to predict not only the electrochemical performance but also the thermal hazard status for optimum cooling systems.

To achieve this purpose, we attempt to build a thermo-electrochemical model of an 18.5 V/50 Ah module with five 50 Ah LIB cells in series and module parts. To determine both the electrochemical and thermal behavior of the module model, all parameters, such as the chemical diffusion coefficient and exchange current density for electrochemical characteristics, are included in the temperature-dependent functions of the model.

The accuracy of the cell model is verified by comparing the experimental and simulated data for C-rates of 0.5, 1, 2, and 5C at three exterior temperatures of 25°C, 35°C, and 45°C. Then, the module model using the cell model is used to investigate the electrochemical behavior under actual wireless tram driving patterns and thermal abuse conditions.

MATERIALS AND METHODS

Cell Disassembly and Equilibrium Potential Measurement

LIB cells (50 Ah) were dismantled in a dry room where the dew point was maintained below −45°C (**Supplementary Figure S1**) to obtain the anode and cathode electrode sheets. Dimethyl carbonate (DMC) was used to clean the electrodes. After washing for 12 h, the DMC was removed by evaporation in a vacuum oven at 60°C for 12 h. The dried cathode and anode electrodes with coating on both sides were used to fabricate coin-type half cells after eliminating the electrode layer coated on one side (**Supplementary Figure S2**). In the case of cathode half-cells, the first cycle was run at 0.1C for solid electrolyte interphase formation, while the next three cycles were run at 0.2C to stabilize the cells at a cutoff voltage of 3.0–4.3 V vs. Li/Li$^+$ (**Supplementary Figure S3A**). For the anode half-cells, similar formation and stabilization processes were conducted at 0.1C and a cutoff voltage of 0.005–1.5 V vs. Li/Li$^+$ (**Supplementary Figure S3B**). Hence, each equilibrium potential for the cathode and anode can be measured at low C-rates of 0.01 and 0.1C for the cathode and anode half-cells, respectively (**Supplementary Figures S3C,D**).

### Composition Analysis of Electrode Active Materials

The compositions of the cathode and anode electrodes were confirmed by energy-dispersive X-ray spectroscopy. From the relative atomic ratio of Ni, Co., and Mn of 4:4:2, the cathode active material was considered to be $LiNi_{0.4}Co_{0.4}Mn_{0.2}O_2$. Similarly, since no peaks other than C were observed in the anode, we assumed that the anode active material was graphite (**Supplementary Figure S4**).

Rate Capability and Temperature Measurement of 50 Ah Cells

We evaluated the rate capability of 50 Ah cells by changing the C-rates from 0.5 to 5C at exterior temperatures of 25°C, 35°C, and 45°C using a cycler capable of 300 A current (PEBC05-300, PNE). In each rate capability test, the temperatures on the cell surface and in the chamber were recorded for comparison with the corresponding simulated data.

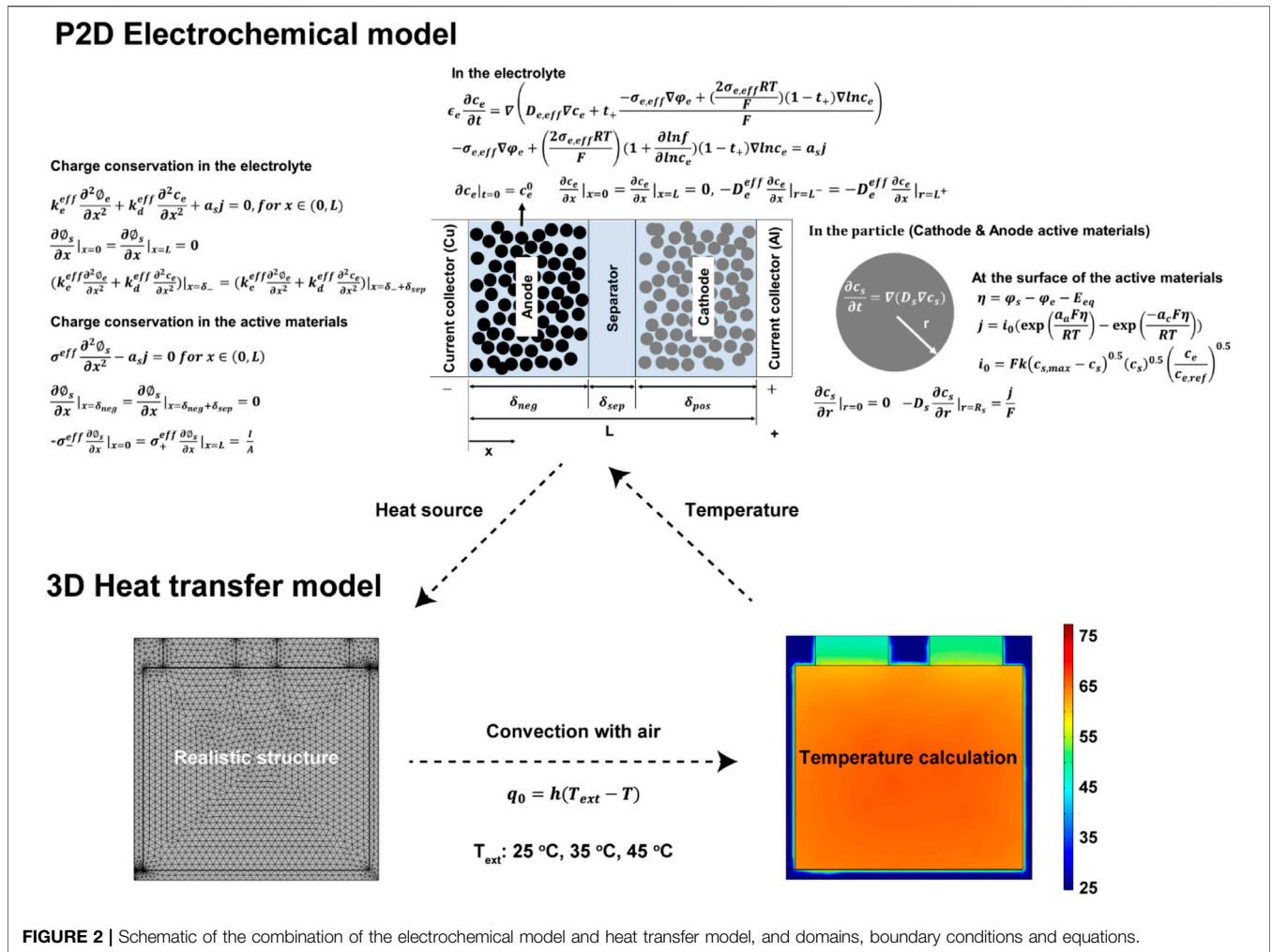### Development of a Thermo-Electrochemical Cell and Module Model

We developed thermo-electrochemical models of the cell and battery module using COMSOL Multiphysics 5.5. The
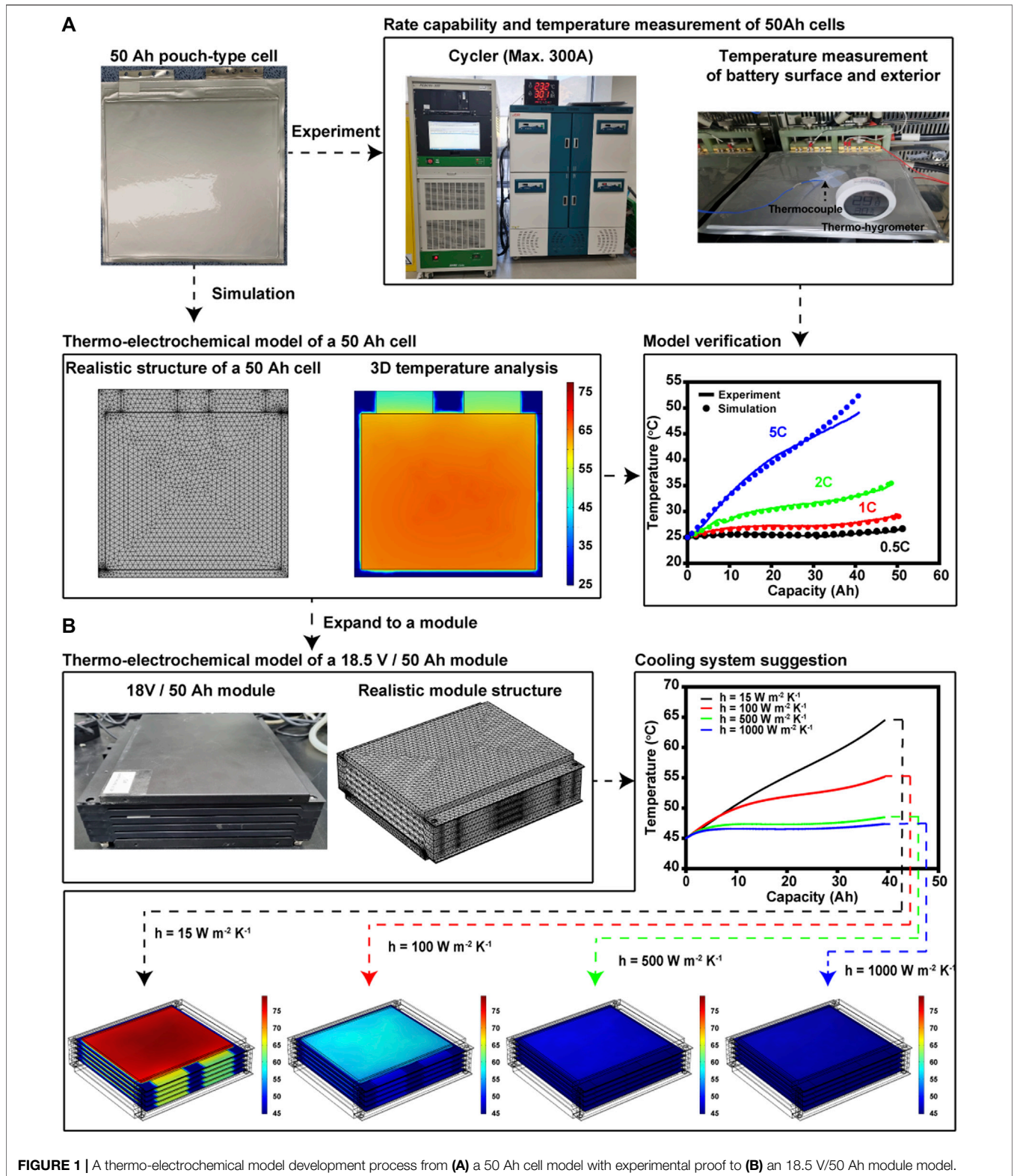
FIGURE 1 | A thermo-electrochemical model development process from **(A)** a 50 Ah cell model with experimental proof to **(B)** an 18.5 V/50 Ah module model.

structures of both the cell (**Figure 1A**) and battery module are almost identical to the real structures (**Figure 1B**). The battery module has five cells, and natural convection is allowed near the module, as in the experimental conditions. We assumed that the five cells released the same heat source during cycling.

FIGURE 2 | Schematic of the combination of the electrochemical model and heat transfer model, and domains, boundary conditions and equations.

RESULTS AND DISCUSSION

Thermo-Electrochemical Model of a 50 Ah Cell

### Combination of Electrochemical Model and Heat Transfer Model of a 50 Ah Cell

The pseudo two-dimensional (P2D) electrochemical model was developed by applying the governing equations and boundary conditions (**Figure 2**; **Supplementary Table S1**). For the heat transfer model, a realistic structure of a 50 Ah cell was formed and assumed to be in contact with the circulated air maintained at specific temperatures. The heat source calculated by the P2D electrochemical model was applied to the 3D electrode structure. The heat transfer model simulated the cell temperature using the heat source and heat transfer through air convection. The calculated temperature returns to the P2D electrochemical model (**Figure 2**). The geometric, electrochemical, and thermal parameters were obtained by dismantling the cell, performing electrochemical measurements, and in previous studies (**Supplementary Table S2**) (Ye et al., 2012; Burheim et al., 2014; Vishwakarma and Jain, 2014; Xu and Wang, 2017; Jaguemont et al., 2019; Keil and Jossen, 2020).

Model Verification: Electrochemical Performance and Surface Temperature a 50 Ah Cell

The electrochemical parameters that significantly affect the cell temperature are the diffusion coefficient and exchange current density, both of which are dependent on the SOL. Therefore, both the equations of the diffusion coefficient and exchange current density were built as functions of the temperature and SOL (**Supplementary Table S3**). As a result, we can illustrate the behaviors of the diffusion coefficient and exchange current density while changing the exterior temperatures and C-rates, as shown in **Figure 3**. As the discharge progressed, the exchange current density of the cathode tended to decrease (**Figure 3A**), while that of the anode increased owing to each SOL (**Figure 3B**). A favorable electrochemical reaction in the cathode occurred at a lower SOL range, and vice versa in the anode. The higher cell temperature caused by the exterior temperature and high C-rate leads to a higher exchange current density for both electrodes. The diffusion coefficients are also dependent on the SOL and temperature, similar to the exchange current density (**Figures 3C,D**). A lower SOL and higher temperature cause the lithium ions to diffuse easily within the electrode active materials.
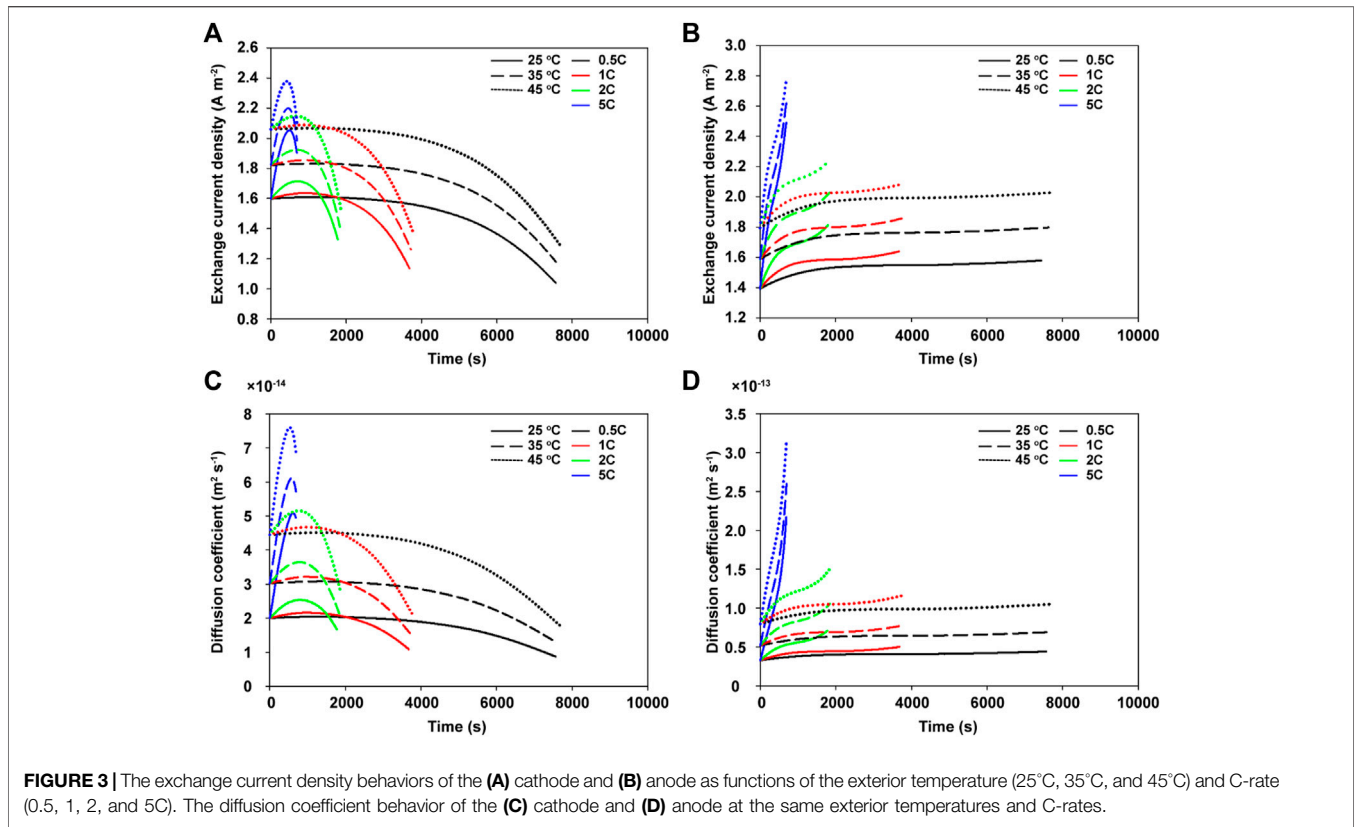
FIGURE 3 | The exchange current density behaviors of the **(A)** cathode and **(B)** anode as functions of the exterior temperature (25°C, 35°C, and 45°C) and C-rate (0.5, 1, 2, and 5C). The diffusion coefficient behavior of the **(C)** cathode and **(D)** anode at the same exterior temperatures and C-rates.
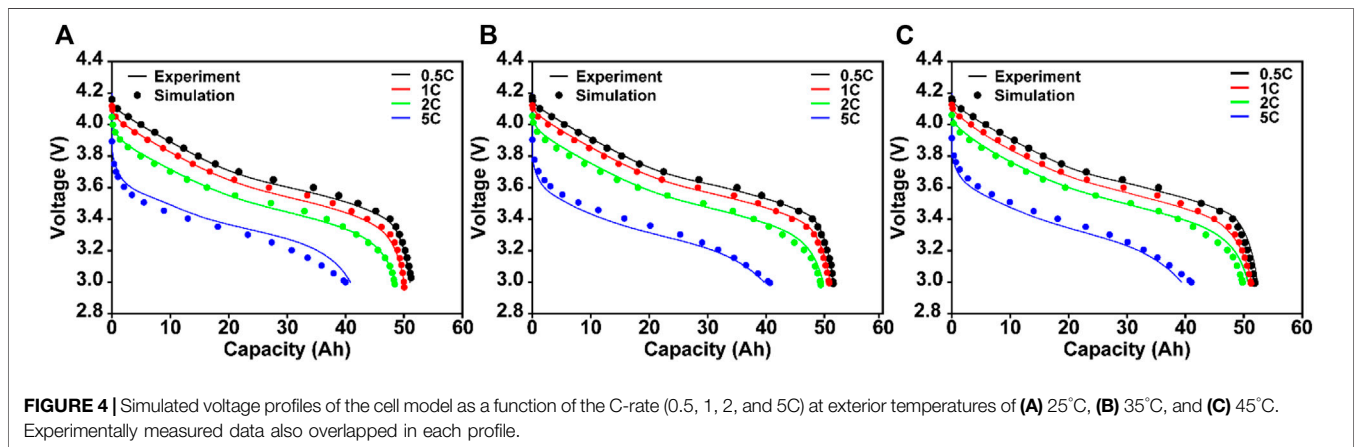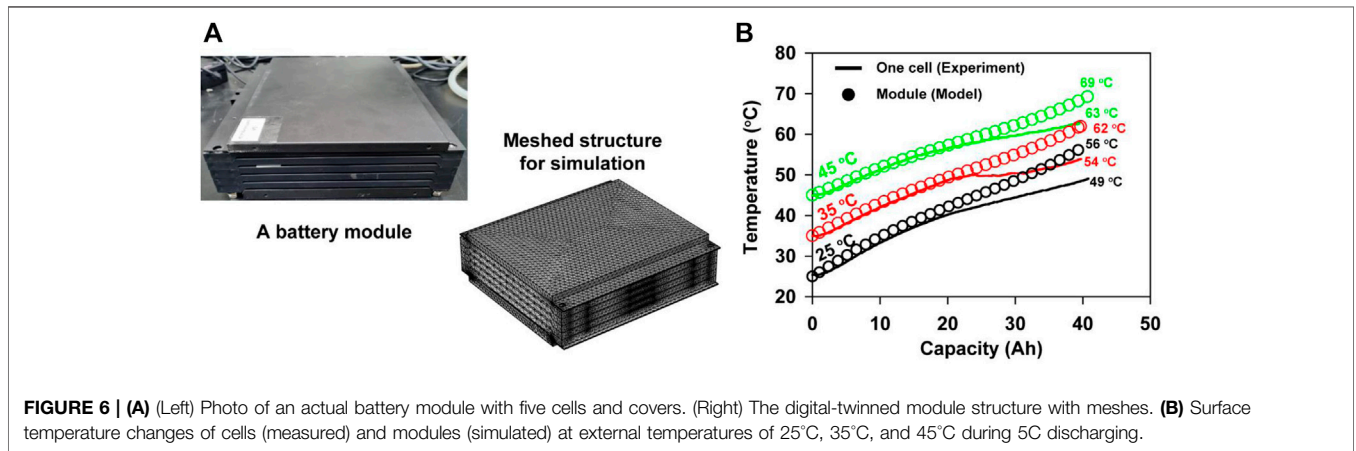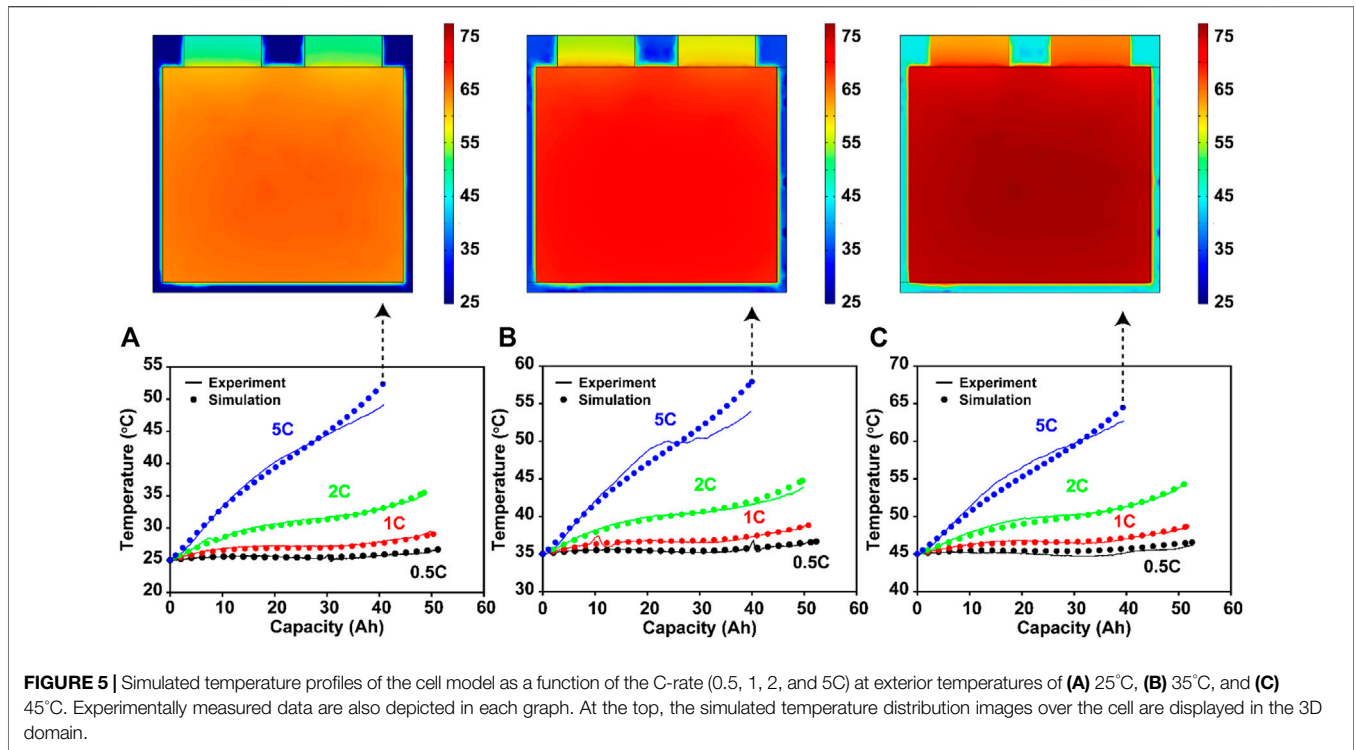

FIGURE 4 | Simulated voltage profiles of the cell model as a function of the C-rate (0.5, 1, 2, and 5C) at exterior temperatures of **(A)** 25°C, **(B)** 35°C, and **(C)** 45°C. Experimentally measured data also overlapped in each profile.

The reliability of our cell model was confirmed by comparing the simulated capacity values, voltage profiles, and temperatures with the experimentally measured values. As summarized in **Figure 4**, the simulated voltage profiles showed good agreement with the experimental results at various C-rate and temperature conditions because both the exchange current density values and diffusion coefficients were well formulated by the cell model, as shown in **Figure 3**. More specifically, our cell model achieved an accuracy of over 98% even at 5C over a wide temperature range [98.47% (**Figure 4A**), 98.96% (**Figure 4B**), and 98.92% (**Figure 4C**) at exterior temperatures of 25°C, 35°C, and 45°C, respectively].

The simulated surface temperatures of the cell model were compared with the experimental measurements, as shown in

Figure 5. Because the heat source caused by electrochemical reactions (**Supplementary Figure S5**) and the heat transfer through convection were well simulated at various C-rates and exterior temperature conditions, the accuracy was high, similar to the simulated capacity values and voltage profiles. For instance, even at 5C (the most extreme case) the simulated temperatures of 25°C, 35 and 45°C showed high accuracy of 97.89% (**Figure 5A**), 97.05% (**Figure 5B**), and 98.44% (**Figure 5C**), respectively. Our cell model can also estimate the overall temperature distribution in the 3D cell structure, including the pouch package, as shown in **Figure 5** (top). However, tab heating caused by internal resistance was excluded because information on the welding condition was not available.
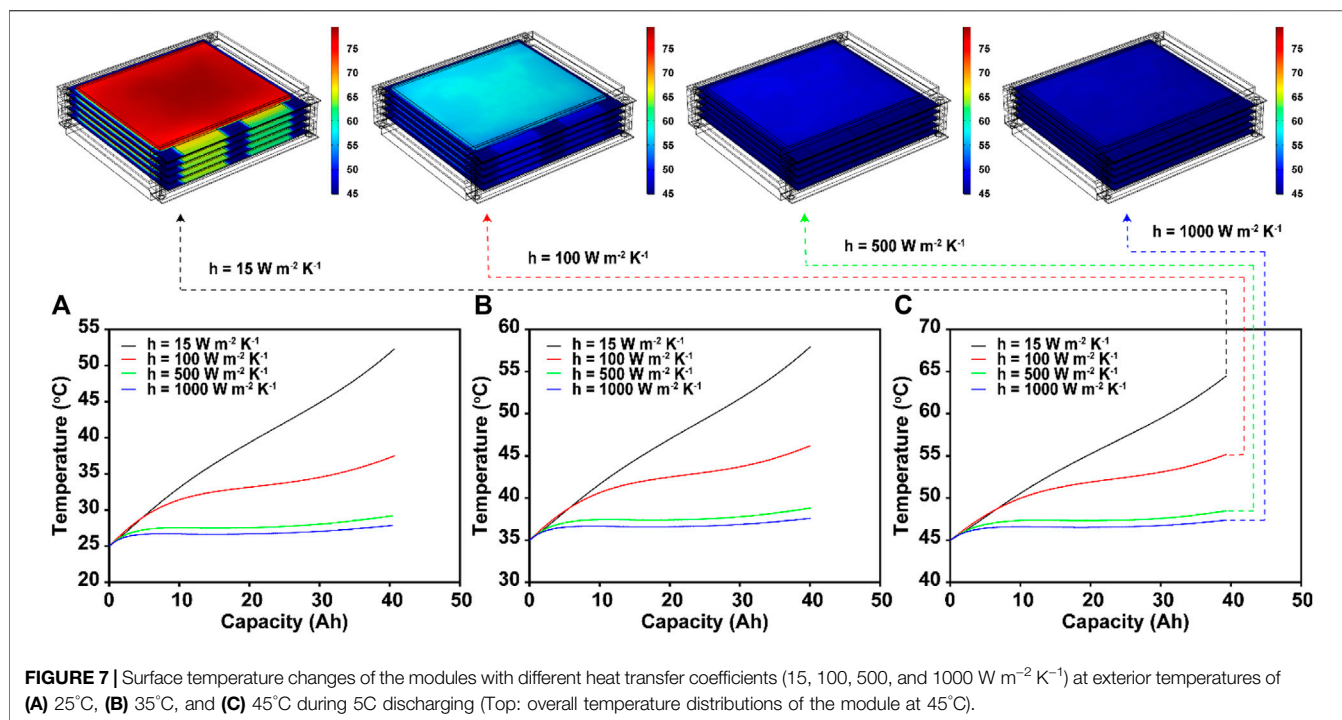
FIGURE 5 | Simulated temperature profiles of the cell model as a function of the C-rate (0.5, 1, 2, and 5C) at exterior temperatures of **(A)** 25°C, **(B)** 35°C, and **(C)** 45°C. Experimentally measured data are also depicted in each graph. At the top, the simulated temperature distribution images over the cell are displayed in the 3D domain.

FIGURE 6 | (A) (Left) Photo of an actual battery module with five cells and covers. (Right) The digital-twinned module structure with meshes. **(B)** Surface temperature changes of cells (measured) and modules (simulated) at external temperatures of 25°C, 35°C, and 45°C during 5C discharging.

Development of Thermo-Electrochemical Model of an 18.5 V/50 Ah Model

Based on a verified cell model, we built a thermo-electrochemical model of a module with five cells, as shown in **Figure 6A**, based on the following assumptions: 1) All the cells have the same initial characteristics such as cell dimensions, capacity, and heat capacity. 2) The same current flows through all the cells with no contact resistance between cells. 3) All the cells were cooled with the same convection efficiency.

Once the heat source is calculated for one cell using the P2D electrochemical cell model, it can be assigned to all the cells. As a result, the temperature changes of the module were simulated as shown in **Figure 6B**, where the average temperatures displayed as the discharge at 5C progressed at exterior temperatures of 25, 35,

and 45°C. At the beginning of the discharge, regardless of the exterior temperature, both the cell and module exhibit similar behaviors of temperature increase. However, after an approximately 20 Ah discharge, the module temperature began to increase more rapidly than the cell temperature owing to the module covers, which may interfere with the heat dissipation from the cell surface to the air. As a result, the final temperatures of the modules (56°C, 62°C, and 69°C) were higher than those of the cells (49°C, 54°C, and 63°C) as shown in **Figure 6B**. The differences ranged from 6 to 8°C regardless of the exterior temperature. Thus, considering the operating temperature range of −30–52°C recommended by the United States Advanced Battery Consortium (USABC) for BEVs, the exterior temperature of 25 °C is an unsafe condition without the

FIGURE 7 | Surface temperature changes of the modules with different heat transfer coefficients (15, 100, 500, and 1000 W m^{-2} K^{-1}) at exterior temperatures of **(A)** 25°C, **(B)** 35°C, and **(C)** 45°C during 5C discharging (Top: overall temperature distributions of the module at 45°C).

appropriate cooling system (Cherry, 2016). In particular, at the exterior temperature of 45°C, the maximum temperature of 69°C exceeds the maximum survival temperature of 66°C set by the USABC. Therefore, cooling systems are essential to control the maximum temperature of the module in this study.

Cooling Systems for 18.5 V/50 Ah-Battery Module

Designing a cooling system requires quantifying the amount of additional heat that must be transferred to the surroundings. Based on the fitted heat transfer coefficient of 15 W m^{-2} K^{-1} in the thermo-electrochemical cell model, the coefficient was increased to 100, 500, and 1000 W m^{-2} K^{-1} in the module model at exterior temperatures of 25°C (**Figure 7A**), 35°C (**Figure 7B**) and 45°C (**Figure 7C**). As shown in **Figure 7**, a minimum of ~100 W m^{-2} K^{-1} is required to keep the maximum temperature of the module below the highest operating temperature set by the USABC (Cherry, 2016). Thus, for the safer and more reliable operation of the module, we simulated the control of the module temperature with a maximum heat transfer coefficient of 500 W m^{-2} K^{-1}, which is theoretically available under forced convection with air (Kosky et al., 2021). Regardless of the exterior temperature, all the temperatures in all cases were maintained within 4°C. However, because the space inside the module is limited and the parts of the module cover prevent air from flowing through the module, this cannot be achieved in a practical manner (Park and Jung, 2013). In this context, coolants with higher heat capacities should be considered for actual battery module or pack systems. Among them, some phase change materials that can remove up to 3000 W m^{-2} K^{-1} of heat have been considered in previous studies (Merlin et al., 2016; Zou et al., 2019; Nie et al., 2020). To examine these situations, we simulated the temperature changes under the same conditions

with a coefficient of 1000 W m^{-2} K^{-1}. As expected, compared with the 500 W m^{-2} K^{-1} case, no significant enhancement was observed: only 1°C was additionally controlled.

Temperature Changes Under an Actual Driving Pattern of Railway Vehicles

Contrary to the case study in *Temperature Changes Under an Actual Driving Pattern of Railway Vehicles*, it is also useful to validate our module model under real driving patterns at 25°C. Based on a power pattern for a real tram operated in Turkey (**Figure 8A**) (Han et al., 2018), we built a driving current pattern for our module, as shown in **Figure 8B**, by considering the total number of cells of 1,076 and single cell capacity of 40 Ah. In this pattern, although the maximum C-rate reached 4C, most of the C-rates were maintained below 1C. As a result, the temperatures of the actual cell, cell model, and module model had similar changes without big differences (**Figure 8C**). Thus, our thermo-electrochemical models for cells and modules are reliable and can be utilized under normal and extreme operating conditions.

CONCLUSION

To assess and control the risks posed by the heat generated by battery modules for wireless railway vehicles, we built a thermo-electrochemical model for an 18.5 V/50 Ah module with five lithium-ion cells (3.7 V/50 Ah). First, a single cell model was developed with an accuracy of over 97% in terms of the capacity values, voltage profiles, and temperature changes under three exterior temperature (25°C, 35°C, and 45°C) and four C-rate (0.5, 1, 2, and 5C) conditions. Then, the cell model was utilized to build
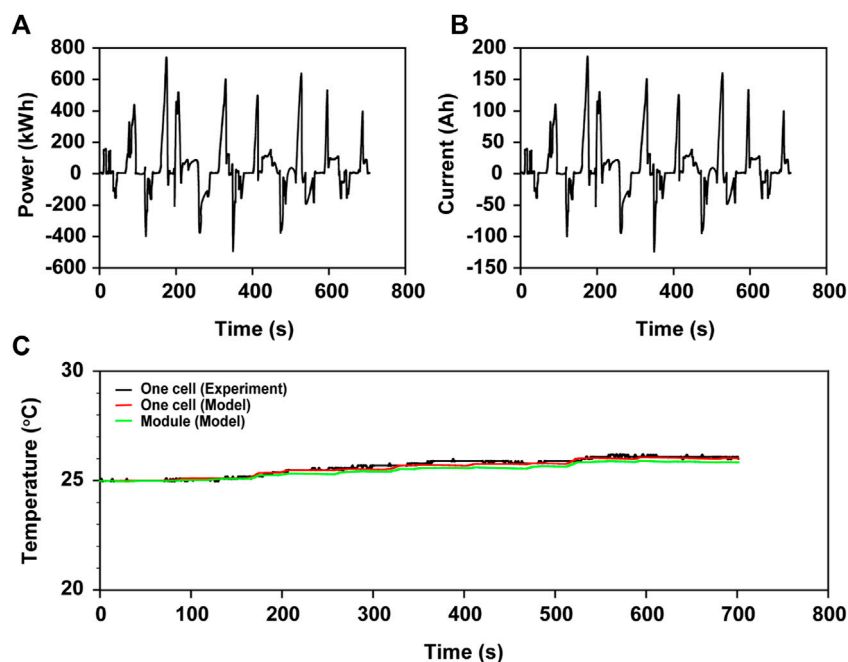
FIGURE 8 | (A) A driving power pattern of a real tram operated in Turkey. **(B)** A revised current pattern for the cell and module in this work. **(C)** Temperature changes of the cell (measured), cell model (simulated), and module model (simulated) under the revised current pattern.

the 18.5 V/50 Ah module model with cover parts. Comparison of the simulated temperature changes of the module with that of the single cell showed that the temperature of the module could exceed 6°C during the 5C discharging condition regardless of the exterior temperature. Furthermore, the maximum temperature of the module of 25°C during the 5C discharging process was expected to increase beyond the highest operating temperature of 52°C set by the USABC. Therefore, it was necessary to determine the amount of heat to be removed. With our module model, we proposed the minimum heat transfer coefficient for cooling systems. Under the driving pattern acquired by a real wireless tram operated in Turkey, not only the cell but also the module maintained its temperature within 3°C. Nonetheless, some unexpected or extreme accidental cases should be considered for risk management. For this purpose, thermo-electrochemical models for modules should be developed and investigated continuously with state-of-the-art large-format and high energy density lithium-ion cells.

DATA AVAILABILITY STATEMENT

The original contributions presented in the study are included in the article/**Supplementary Material**, further inquiries can be directed to the corresponding authors.

AUTHOR CONTRIBUTIONS

JS: Formal analysis, Investigation, Methodology, Software, Visualization, Writing—original draft. HyL: Methodology, Formal analysis. SK: Formal analysis. DK: Investigation. SJ: Visualization. HoL: Project administration. T-SK: Resource, Funding acquisition. YL: Supervision, Conceptualization, Methodology, Investigation, Writing—review and editing, Project administration.

FUNDING

ACKNOWLEDGMENTS

SUPPLEMENTARY MATERIAL

The Supplementary Material for this article can be found online at: https://www.frontiersin.org/articles/10.3389/fmats.2022.824168/full#supplementary-material

REFERENCES

Bahiraei, F., Fartaj, A., and Nazri, G.-A. (2017). Electrochemical-thermal Modeling to Evaluate Active Thermal Management of a Lithium-Ion Battery Module. *Electrochimica Acta* 254, 59–71. doi:10.1016/j.electacta.2017.09.084

Basu, S., Hariharan, K. S., Kolake, S. M., Song, T., Sohn, D. K., and Yeo, T. (2016). Coupled Electrochemical thermal Modelling of a Novel Li-Ion Battery Pack thermal Management System. *Appl. Energ.* 181, 1–13. doi:10.1016/j.apenergy.2016.08.049

Burheim, O. S., Onsrud, M. A., Pharoah, J. G., Vullum-Bruer, F., and Vie, P. J. S. (2014). Thermal Conductivity, Heat Sources and Temperature Profiles of Li-Ion Batteries. *ECS Trans.* 58, 145–171. doi:10.1149/05848.0145ecst

Chen, S. C., Wan, C. C., and Wang, Y. Y. (2005). Thermal Analysis of Lithium-Ion Batteries. *J. Power Sourc.* 140, 111–124. doi:10.1016/j.jpowsour.2004.05.064

Chen, Y., and Evans, J. W. (1993). Heat Transfer Phenomena in Lithium/Polymer-Electrolyte Batteries for Electric Vehicle Application. *J. Electrochem. Soc.* 140, 1833–1838. doi:10.1149/1.2220724

Chen, Y., and Evans, J. W. (1994). Three-Dimensional Thermal Modeling of Lithium-Polymer Batteries under Galvanostatic Discharge and Dynamic Power Profile. *J. Electrochem. Soc.* 141, 2947–2955. doi:10.1149/1.2059263

Cherry, J. (2016). *Battery Durability in Electrified Vehicle Applications: A Review of Degradation Mechanisms and Durability Testing. FEV* Final Report EP-C-12-014 Wa 3-01, 1.

Ciccarelli, F., Del Pizzo, A., and Iannuzzi, D. (2014). Improvement of Energy Efficiency in Light Railway Vehicles Based on Power Management Control of Wayside Lithium-Ion Capacitor Storage. *IEEE Trans. Power Electron.* 29, 275–286. doi:10.1109/tpel.2013.2253492

Feng, X., Ouyang, M., Liu, X., Lu, L., Xia, Y., and He, X. (2018). Thermal Runaway Mechanism of Lithium Ion Battery for Electric Vehicles: A Review. *Energ. Storage Mater.* 10, 246–267. doi:10.1016/j.ensm.2017.05.013

Gu, W. B., and Wang, C. Y. (2000). Thermal-electrochemical Modeling of Battery Systems. *J. Electrochem. Soc.* 147, 2910. doi:10.1149/1.1393625

Guo, M., Sikha, G., and White, R. E. (2011). Single-Particle Model for a Lithium-Ion Cell: Thermal Behavior. *J. Electrochem. Soc.* 158, A122. doi:10.1149/1.3521314

Han, Y., Li, Q., Wang, T., Chen, W., and Ma, L. (2018). Multisource Coordination Energy Management Strategy Based on SOC Consensus for a PEMFC-Battery-Supercapacitor Hybrid Tramway. *IEEE Trans. Veh. Technol.* 67, 296–305. doi:10.1109/tvt.2017.2747135

Jaguemont, J., Sokkeh, M., Hosen, S., Jin, L., Qiao, G., Kalogiannis, T., et al. (2019). "1D-Thermal Analysis and Electro-Thermal Modeling of Prismatic-Shape LTO and NMC Batteries," in 2019 IEEE Vehicle Power and Propulsion Conference (VPPC), 1–5.

Jeong, M. G., Cho, J.-H., and Lee, B. J. (2019). Heat Transfer Analysis of a High-Power and Large-Capacity thermal Battery and Investigation of Effective thermal Model. *J. Power Sourc.* 424, 35–41. doi:10.1016/j.jpowsour.2019.03.067

Keil, J., and Jossen, A. (2020). Electrochemical Modeling of Linear and Nonlinear Aging of Lithium-Ion Cells. *J. Electrochem. Soc.* 167, 110535. doi:10.1149/1945-7111/aba44f

Kim, S. U., Albertus, P., Cook, D., Monroe, C. W., and Christensen, J. (2014). Thermoelectrochemical Simulations of Performance and Abuse in 50-Ah Automotive Cells. *J. Power Sourc.* 268, 625–633. doi:10.1016/j.jpowsour.2014.06.080

Konishi, T., and Tobita, M. (2012). "Fixed Energy Storage Technology Applied for DC Electrified Railway (Traction Power Substation)", in: 2012 Electrical Systems for Aircraft, Railway and Ship Propulsion), 1–6.doi:10.1109/esars.2012.6387438

Kosky, P., Balmer, R., Keat, W., and Wise, G. (2021). "Mechanical Engineering," in *Exploring Engineering*. Editors P. Kosky, R. Balmer, W. Keat, and G. Wise. Fifth Edition (Academic Press), 317–340. doi:10.1016/b978-0-12-815073-3.00014-4

Kumaresan, K., Sikha, G., and White, R. E. (2008). Thermal Model for a Li-Ion Cell. *J. Electrochem. Soc.* 155, A164. doi:10.1149/1.2817888

Lai, Y., Du, S., Ai, L., Ai, L., Cheng, Y., Tang, Y., et al. (2015). Insight into Heat Generation of Lithium Ion Batteries Based on the Electrochemical-thermal Model at High Discharge Rates. *Int. J. Hydrogen Energ.* 40, 13039–13049. doi:10.1016/j.ijhydene.2015.07.079

Liang, J., Gan, Y., Li, Y., Tan, M., and Wang, J. (2019). Thermal and Electrochemical Performance of a Serially Connected Battery Module Using a Heat Pipe-Based thermal Management System under Different Coolant Temperatures. *Energy* 189, 116233. doi:10.1016/j.energy.2019.116233

Liang, J., Gan, Y., Tan, M., and Li, Y. (2020). Multilayer Electrochemical-thermal Coupled Modeling of Unbalanced Discharging in a Serially Connected Lithium-Ion Battery Module. *Energy* 209, 118429. doi:10.1016/j.energy.2020.118429

Merlin, K., Delaunay, D., Soto, J., and Traonvouez, L. (2016). Heat Transfer Enhancement in Latent Heat thermal Storage Systems: Comparative Study of Different Solutions and thermal Contact Investigation between the Exchanger and the PCM. *Appl. Energ.* 166, 107–116. doi:10.1016/j.apenergy.2016.01.012

Nie, B., Zou, B., She, X., Zhang, T., Li, Y., and Ding, Y. (2020). Development of a Heat Transfer Coefficient Based Design Method of a thermal Energy Storage Device for Transport Air-Conditioning Applications. *Energy* 196, 117083. doi:10.1016/j.energy.2020.117083

Okui, A., Hase, S., Shigeeda, H., Konishi, T., and Yoshi, T. (2010). "Application of Energy Storage System for Railway Transportation in Japan", in: The 2010 International Power Electronics Conference - ECCE ASIA -), 3117–3123.

Pals, C. R., and Newman, J. (1995). Thermal Modeling of the Lithium/Polymer Battery: I Discharge Behavior of a Single Cell. *J. Electrochem. Soc.* 142, 3274–3281. doi:10.1149/1.2049974

Park, S., and Jung, D. (2013). Battery Cell Arrangement and Heat Transfer Fluid Effects on the Parasitic Power Consumption and the Cell Temperature Distribution in a Hybrid Electric Vehicle. *J. Power Sourc.* 227, 191–198. doi:10.1016/j.jpowsour.2012.11.039

Rao, L., and Newman, J. (1997). Heat-Generation Rate and General Energy Balance for Insertion Battery Systems. *J. Electrochem. Soc.* 144, 2697–2704. doi:10.1149/1.1837884

Song, L., and Evans, J. W. (2000). Electrochemical-Thermal Model of Lithium Polymer Batteries. *J. Electrochem. Soc.* 147, 2086. doi:10.1149/1.1393490

Srinivasan, V., and Wang, C. Y. (2003). Analysis of Electrochemical and Thermal Behavior of Li-Ion Cells. *J. Electrochem. Soc.* 150, A98–A106. doi:10.1149/1.1526512

Verbrugge, M. W. (1995). Three-dimensionai Temperature and Current Distribution in a Battery Module. *Aiche J.* 41, 1550–1562. doi:10.1002/aic.690410619

Vishwakarma, V., and Jain, A. (2014). Measurement of In-Plane thermal Conductivity and Heat Capacity of Separator in Li-Ion Cells Using a Transient DC Heating Method. *J. Power Sourc.* 272, 378–385. doi:10.1016/j.jpowsour.2014.08.066

Wang, G., Gao, Q., Yan, Y., and Zhang, Y. (2021). Transient Process Optimization of Battery Cooling on Heat Transfer Enhancement Structure. *Appl. Therm. Eng.* 182, 115897. doi:10.1016/j.applthermaleng.2020.115897

Wu, W., Xiao, X., and Huang, X. (2012). The Effect of Battery Design Parameters on Heat Generation and Utilization in a Li-Ion Cell. *Electrochimica Acta* 83, 227–240. doi:10.1016/j.electacta.2012.07.081

Xu, M., and Wang, X. (2017). Electrode Thickness Correlated Parameters Estimation for a Li-Ion NMC Battery Electrochemical Model. *ECS Trans.* 77, 491–507. doi:10.1149/07711.0491ecst

Ye, Y., Shi, Y., Cai, N., Lee, J., and He, X. (2012). Electro-thermal Modeling and Experimental Validation for Lithium Ion Battery. *J. Power Sourc.* 199, 227–238. doi:10.1016/j.jpowsour.2011.10.027

Zhao, J., Rao, Z., Huo, Y., Liu, X., and Li, Y. (2015). Thermal Management of Cylindrical Power Battery Module for Extending the Life of New Energy Electric Vehicles. *Appl. Therm. Eng.* 85, 33–43. doi:10.1016/j.applthermaleng.2015.04.012

Zou, D., Liu, X., He, R., Zhu, S., Bao, J., Guo, J., et al. (2019). Preparation of a Novel Composite Phase Change Material (PCM) and its Locally Enhanced Heat Transfer for Power Battery Module. *Energ. Convers. Management* 180, 1196–1202. doi:10.1016/j.enconman.2018.11.064

Conflict of Interest: The authors declare that the research was conducted in the absence of any commercial or financial relationships that could be construed as a potential conflict of interest.

Publisher's Note: All claims expressed in this article are solely those of the authors and do not necessarily represent those of their affiliated organizations, or those of the publisher, the editors and the reviewers. Any product that may be evaluated in this article, or claim that may be made by its manufacturer, is not guaranteed or endorsed by the publisher.